Bioorganic & Medicinal Chemistry Letters 20 (2010) 6998–7003

Contents lists available at ScienceDirect

Bioorganic & Medicinal Chemistry Letters

journal homepage: www.elsevier.com/locate/bmcl

Identification of potent ITK inhibitors through focused compound library design including structural information

Matthias Herdemann [†], Isabelle Heit [*], Frank-Uwe Bosch, Gianluca Quintini, Claudia Scheipers [‡], Alexander Weber [§,*]

Nycomed GmbH, Byk-Gulden-Str. 2, D-78467 Konstanz, Germany

ARTICLE INFO

Article history:
Received 8 August 2010
Revised 23 September 2010
Accepted 24 September 2010
Available online 29 September 2010

Keywords:
ITK
Interleukin-2 inducible T cell kinase
ITK inhibitors
Library design
Kinases
Drug design
Docking
Crystal structure
X-ray
Lead finding
Lead optimisation
Focused kinase library
Ligand efficiency

ABSTRACT

A series of novel compound libraries inhibiting interleukin-2 inducible T cell kinase (ITK) were designed, synthesized and evaluated. In the first design cycle two library scaffolds were identified showing low micromolar inhibition of ITK. Further iterative design cycles including crystal structure information of ITK and structurally related kinases led to the identification of indolylindazole and indolylpyrazolopyridine compounds with low nanomolar ITK inhibition.

Interleukin-2 inducible T cell kinase (ITK) is a member of the Tec family of non-receptor tyrosine kinases and is mainly expressed in T cells, mast cells and natural killer cells.[1] In T cells, ITK is activated after T cell receptor (TCR) stimulation leading to IL-2 production, proliferation and differentiation.[2] In studies with ITK$^{-/-}$ mice reduced lung inflammation and impaired T cell response were observed in an ovalbumin-induced allergic asthma model.[3] Similar results were reported with a selective ITK inhibitor[4] indicating the important role of ITK kinase activity in inflammatory processes. Therefore, inhibiting ITK should be an attractive approach to interfere with the pathogenesis of T cell-mediated diseases.

Here, we report the design of new ITK inhibitors obtained within an ITK hit identification project. Our initial focused library design approach included structural information provided by X-ray structure of ITK in complex with Staurosporine,[5] as well as in-depth analysis of published ITK inhibitors (Fig. 1) which were docked into the ATP binding pocket of ITK. The aim of the project was the design of novel hit structures which would represent a promising starting point for subsequent lead finding and lead optimisation. The newly designed scaffolds should possess high potency on enzyme inhibition combined with favourable physicochemical properties. Furthermore, the expected synthetic feasibility of the new libraries were taken into consideration to ensure that subsequent chemical modifications should be easy to address in following optimisation steps. In addition, within the first design cycle we focus on small lead-like compounds[6] and therefore restricted the molecular weight of the synthesized compounds to 350 Da. Expecting low micromolar inhibition within this first series, the ligand efficiency (LE, calculated binding energy per non-hydrogen atom)[7] of these compounds will be greater than 0.3, serving as a good starting point for further optimisations.[8] Furthermore, the published X-ray structure of ITK in complex with Staurosporine[5] was used to support the library design concept to identify most favourable interactions within the protein. Reference compounds[9] with known ITK inhibitory activity (Fig. 1) were docked and minimised in the ITK ATP binding pocket (PDB

* Corresponding authors. Tel.: +49 7531 84 3130; fax: +49 7531 84 93130 (I.H.).
E-mail addresses: isabelle.heit@nycomed.com (I. Heit), alexander.weber@boehringer-ingelheim.com (A. Weber).
† Present address: EPO, Patentlaan 3-9, 2288 EE The Hague, Netherlands.
‡ Present address: Intervet Innovation GmbH, Zur Probstei, 55270 Schwabenheim, Germany.
§ Present address: Boehringer Ingelheim Pharma GmbH & Co. KG, Birkendorfer Straße 65, 88397 Biberach an der Riß, Germany.

0960-894X/$ - see front matter © 2010 Elsevier Ltd. All rights reserved.
doi:10.1016/j.bmcl.2010.09.119

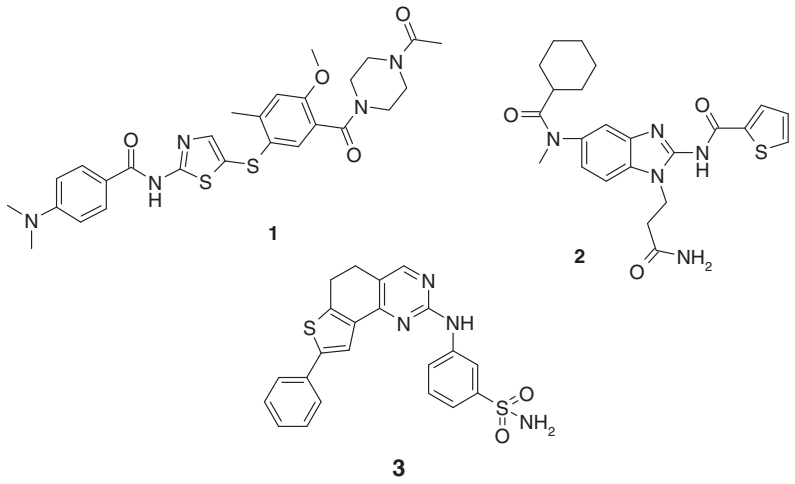

Figure 1. Published ITK inhibitors included in focused library design approach.

code: 1sm2),[10] leading to a superposition of the most interesting structural classes that are known to influence ITK activity. Both the crystal structure of ITK in complex with Staurosporine and the docked conformations of reference ligands in ITK lead to the identification of main protein–ligand interactions: (1) hydrogen-bond interactions with backbone carbonyl oxygen of Glu-436 and backbone nitrogen and oxygen of Met-438 in the hinge region (HR), (2) polar interactions with Ser-499 and Asp-500 side chains and (3) aromatic and hydrophobic interactions with the gatekeeper (GK) Phe-435 and a small solvent exposed hydrophobic pocket (Ile-369, Leu-379, Phe-437). Especially, the hydrogen bonding network of ligands towards the hinge region in ITK should be similar compared to structurally related protein–ligand kinase complexes.[11] Published crystal structures of CDK2 with aminothiazole (PDB code: 2btr, 2bts) and aminopyrazole inhibitors (PDB code: 1vyw, 1vyz) show that both inhibitor classes bind to CDK2 forming hydrogen bonds to amino acid backbone atoms in the CDK2 hinge region (Glu-81, Leu-83).[12] A protein-based superposition of those CDK2 X-ray structures with ITK (PDB code: 1sm2) indicate that the hydrogen bonding network of both inhibitor classes towards the hinge region in CDK2 could be formed in ITK, too.

The potency of the library compounds was tested in an in vitro Itk kinase assay using the full-length protein.[15] After the first synthesis cycle indazole and pyrazole derivatives prepared previously by amide coupling of the corresponding commercially available acids were identified with low micromolar ITK inhibition (Fig. 2). The proposed binding mode of both classes based on docking studies in ITK is shown in Figure 3. Both lead-like classes possess excellent physicochemical properties and represent good starting points for further optimisation (MW <350 Da, LE >0.3). A crystal structure of compound **4a** in ITK was not available after the first design cycle, instead a co-crystal structure of indazole **4a** in CDK2 could be observed (data not shown), indicating hydrogen bonding with both indazole nitrogen atoms to the CDK2 hinge region. Compound **4a** (ITK IC_{50} = 5 μM) was tested against CDK2 which revealed that this ligand also inhibits CDK2 in the low micromolar range (CDK2 IC_{50} = 3 μM). Interestingly, the results from docking and minimisation of **4a** in ITK (Fig. 3) indicated that **4a** would not be of entirely planar structure. The docking studies predicted a twist of the aniline's phenyl ring with regard to the indazole-amide moiety. However, it was assumed that for the binding to ITK, but not for CDK2, a more planar inhibitor scaffold would be preferred. We considered that the replacement of the amide function by a five-membered ring, that is, the replacement of the anilide moiety by an indole, would be the most effective approach to obtain compounds of

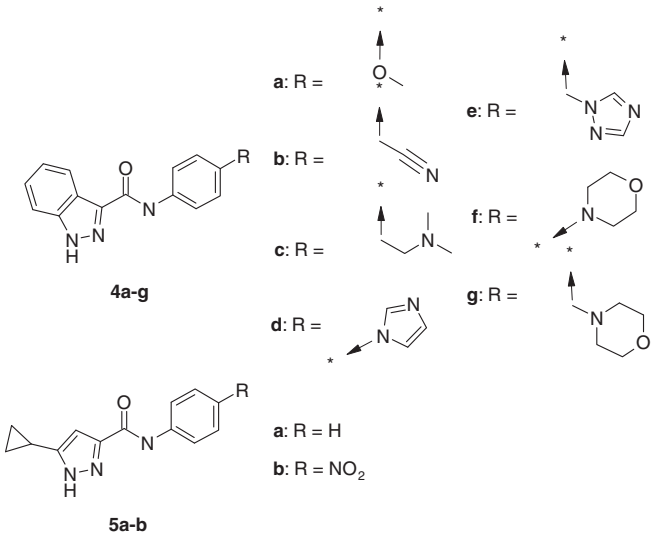

Figure 2. Indazole and pyrazole derivatives identified after first design cycle.

similar size and ligand efficiency. Such compounds would very likely have a planar structure. This approach is illustrated in Scheme 1. The transformation of the amide function of compounds **4** to a five-membered ring of their derivatives **6** and **7** should alter the angle at the amides nitrogen atom. Consequently, the para-substituents of initial hits **4a–g** would have to be attached at position 6 of the indole in order to occupy the same space within the ATP binding pocket. Therefore, the next design cycles were focused on indazole derivatives of structures **6**, as well as on analogous pyrazolopyridines **7**, attempting to increase the affinity towards the target kinase ITK while gaining selectivity towards CDK2.

In order to allow an independent variation of substituents at both moieties of compounds **6** and **7** (Scheme 1), it was decided to combine both heterocyclic fragments in the very last steps of the synthesis. This was done by Suzuki coupling of iodo-indazole **8** or iodo-pyrazolopyridine **9** respectively with the indol-2-ylboronic acids **10** using the [1,1′-bis(diphenylphosphino)ferrocene]palladium(II) complex Pd(dppf)Cl_2–DCM[13] as catalyst and cesium carbonate as a base (Scheme 2). The crude products were then directly deprotected with potassium carbonate in a mixture of water/methanol/THF to give the final compounds **6** and **7**.[16] Compound **6g** (R^1 = H, R^2 = 6-CO_2H) was isolated in 83% overall yield after refluxing the purified

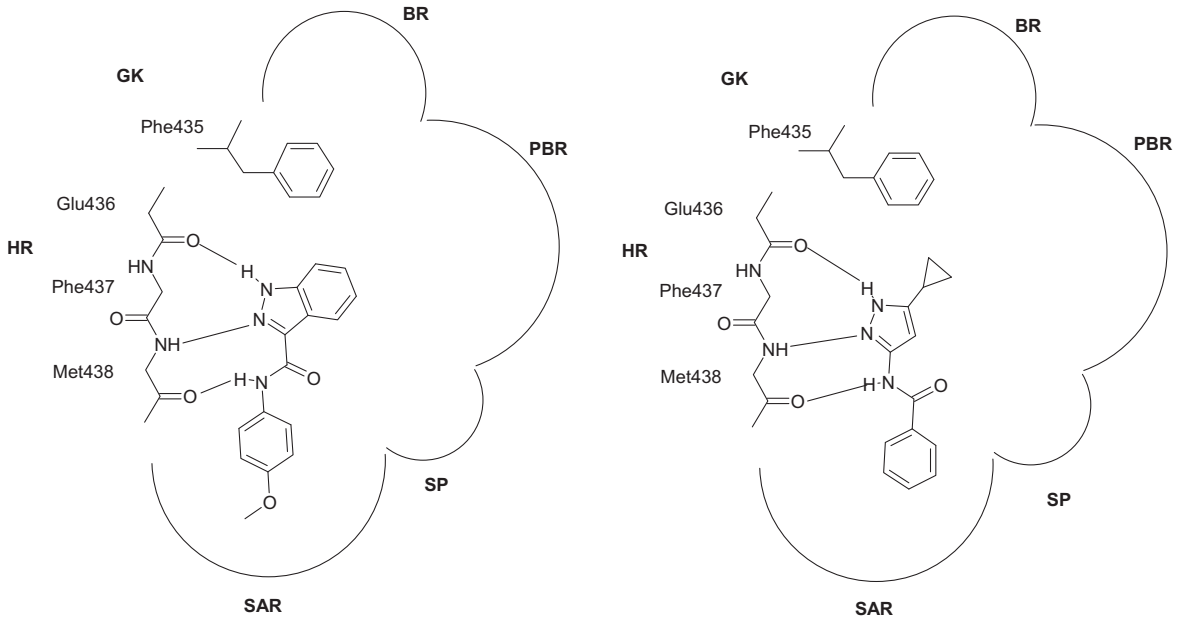

Figure 3. Proposed binding mode of indazole- and pyrazole derivatives in ITK identified after the first design cycle. Hydrogen bonding interactions of compound **4a** (left) and **5a** (right) with the hinge region are shown in dotted lines.

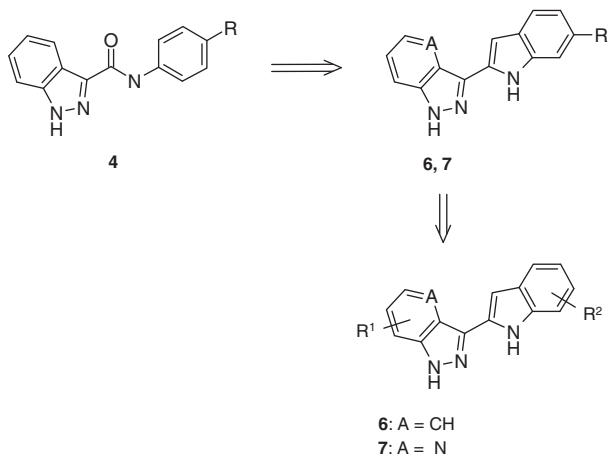

Scheme 1. Second synthesis cycle approach.

intermediate of Suzuki coupling with KOH in ethanol. Under these conditions the methyl carboxylate group was readily cleaved to give the desired acid function after acidic work-up. The building block **9** was synthesized starting from commercial 3-fluoropyridine (Scheme 3). After regioselective deprotonation with *n*BuLi/TMEDA which was prepared in situ, formylation has been achieved with DMF. Intermediate **11** was then converted without purification in two steps to 1*H*-pyrazolo[4,3-*b*]pyridine (**12**). After condensation of the aldehyde with hydrazine the ring closure was achieved at 130 °C. The yield for the entire sequence from 3-fluoropyridine to 1*H*-pyrazolo[4,3-*b*]pyridine (**12**) was 26–30%. Building block **9** was then obtained by regioselective iodination of heterocycle **12** under basic conditions followed by Boc protection (81%). The same reaction conditions as for the transformation of **12** to **9** were applied to commercially available indazoles for the preparation of Boc protected iodo-indazoles **8** (80–95% yield). Those boronic acids **10** which were not commercially available were prepared starting from the corresponding indoles **13** (Scheme 4). After Boc protection the intermediate **14** was reacted with triisopropoxyborane in THF using the base lithium diisopropylamide (LDA). Following work-up, indol-2-ylboronic acids **10** were isolated in 70–80% yield.

The prepared indolylindazoles **6** and indolylpyrazolopyridines **7** were first evaluated in an enzymatic assay using an ITK full-length enzyme.[15] Subsequently, selected compounds were tested for their inhibition of anti-CD3/anti-CD28 induced interleukin-2 (IL-2)

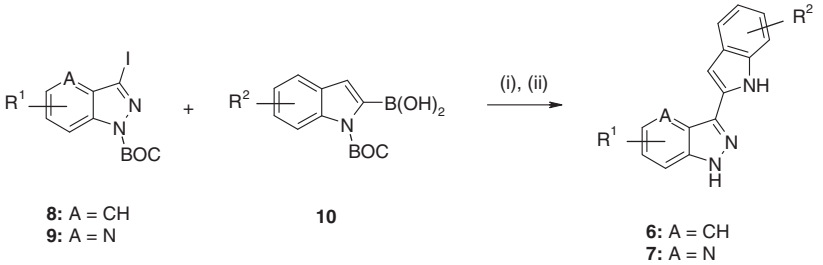

Scheme 2. Reagents and conditions: (i) Pd(dppf)Cl_2–DCM, Cs_2CO_3, dioxane, 80 °C, 2–4 h, argon; (ii) 4 M K_2CO_3aq, MeOH, THF, 60 °C, 3–4 h or KOH, EtOH, reflux, 1 h.

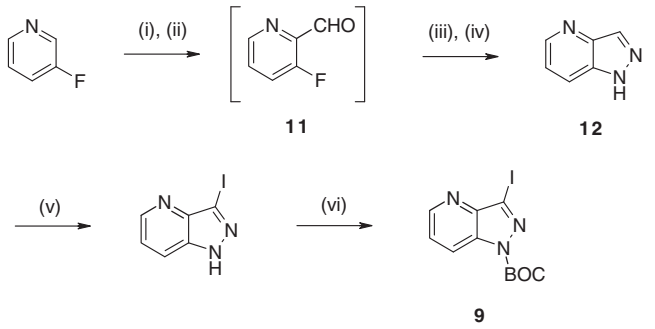

Scheme 3. Reagents and conditions: (i) *n*BuLi/TMEDA, Et_2O, −75 °C, 4 h, argon; (ii) DMF, Et_2O, −75 °C, 2 h under argon; (iii) N_2H_4–H_2O, rt, 18 h; (iv) 130 °C, 5 h; (v) I_2, KOH, DMF, 0 °C to rt, 2.5 h; (vi) Boc_2O, NEt_3, DMAP, DMF, 0 °C to rt, 1 h.

release in primary human CD4+ T cells as relevant cellular system.[17] Within the indolylindazole series, the unsubstituted compound (**6a**) inhibited ITK with an IC_{50} of 140 nM in the enzymatic assay and showed an IC_{50} of 2.3 μM in the cellular assay (Table 1). Similar potency was observed for the derivatives having a methoxy substituent in either position 5 or 6 (**6b** and **6c**). However, as predicted by docking studies, the introduction of a methoxy substituent at position 7 resulted in a dramatic loss of activity. Due to steric restrictions at that position in the ITK binding pocket (Phe-437) the binding affinity of **6d** was significantly reduced (IC_{50} = 22 μM). The potencies observed for **6a**–**c** correspond to a more than 10-fold activity increase compared to those of initial indazole hits **4** (Fig. 2). In particular, while first generation compound **4a** had an enzymatic IC_{50} of 5 μM, the corresponding second generation compound **6c** inhibited ITK enzyme with an IC_{50} of 130 nM (Table 1). A methyl substituent at the indole's positions 5 or 6 led to similar enzymatic activities as methoxy groups (**6e** and **6f**). In contrast, with an IC_{50} of about 4 μM compound **6g** was significantly less active, due to its carboxylic acid function. A similar SAR was observed within the pyrazolopyridine series. Unsubstituted compound **7a** had an enzymatic IC_{50} of 200 nM and exhibited the same potency in the functional assay as **6a** (Table 1). Surprisingly, with an enzymatic IC_{50} of 60 nM **7c** was twofold more potent than the analogous indolylindazole **6c**. However, both compounds possess the same cellular potency of 1.2 μM. Likewise, the enzymatic potency of the 5-methyl derivative **7f** was slightly higher than that of **6f**. Both compounds **6f** and **7f** inhibited IL-2 in the functional assay with an IC_{50} below 1 μM. Furthermore, a bromo substituent was also tolerated in position 6 of the indole, as well in position 4 (**7g** and **7h**). With regard to the indazole moiety of compounds **6**, our initial work was focussed on the positions 5 and 6 (Table 2). Docking studies[10] performed with **4a** (Fig. 3) indicated that the ITK binding pocket should allow substitutions at both positions. A substituent in position 6 could make favourable interactions with gatekeeper Phe-435. However, it should be limited in size to avoid a steric clash with the gatekeeper residue. Testing for the affinity to the target enzyme revealed that methyl and fluoro substituents are tolerated in both positions and do not alter the enzymatic activity (**6k**–**n**). A cyano group, either in position 5 or in 6, increases slightly the enzymatic activity compared to

Table 1
Results of selected indole substitutions

Compound	A	R^1	R^2	IC_{50} (μM) enzyme[a]	IC_{50} (μM) cell, IL-2[a]
6a	CH	H	H	0.14	2.3
6b	CH	H	5-OMe	0.12	4.6
6c	CH	H	6-OMe	0.13	1.2
6d	CH	H	7-OMe	22	—
6e	CH	H	5-Me	0.35	4.1
6f	CH	H	6-Me	0.11	0.7
6g	CH	H	6-CO_2H	3.98	—
7a	N	H	H	0.20	2.2
7b	N	H	5-OMe	0.28	3.2
7c	N	H	6-OMe	0.06	1.4
7d	N	H	7-OMe	27	—
7e	N	H	5-Me	0.30	5.6
7f	N	H	6-Me	0.07	0.9
7g	N	H	4-Br	0.24	—
7h	N	H	6-Br	0.23	—

[a] IC_{50} values are means from two to three independent experiments.

Table 2
Results of selected indazole substitutions

Compound	R^1	R^2	IC_{50} (μM) enzyme[a]	IC_{50} (μM) cell, IL-2
6k	5-Me	H	0.25	—
6l	6-Me	H	0.16	—
6m	5-F	H	0.17	—
6n	6-F	H	0.19	—
6o	5-CN	H	0.08	—
6p	6-CN	H	0.08	—
6q	5-Me	6-Me	0.31	—
6r	6-Me	6-Me	0.09	—
6s	6-F	6-Me	0.14	—
6t	6-CN	6-Me	0.07	—
6u	6-F	6-OMe	0.08	—

[a] IC_{50} values are means from two to three independent experiments.

unsubstituted compound **6a** (**6o** and **6p**). As a further exploration of the initial SAR, as well as a validation of our docking model, substituted indoles were combined with substituted indazole fragments. Both, a 6-methyl and a 6-cyano substituent at the indazole heterocycle enhanced the activity of 6-methyl indolyl compounds (**6r** and **6t**) compared to parent compound **6f**. The same was observed for 6-methoxy indolyl compound (**6u**) with regard to **6c**. As observed for **6k** and **6n** with regard to **6a**, neither the 5-methyl nor the 6-fluoro group changed the activities of **6q** and **6s** compared to **6f**. According to the previously discussed criterion of ligand efficiency the values of representative compounds of the first design cycle (LE = 0.30–0.35) were further improved for compounds of the following cycles, that is, indolylindazoles **6** and indolylpyrazolopyridines **7**. They reached LE values in the range of up to 0.40–0.50.

In view of its promising potency in the enzymatic assay (IC_{50} = 60 nM) compound **7c** was used for in-depth molecular modelling analyses. Figure 4 shows the binding modes of the known benzimidazole ITK inhibitor **2** and pyrazolopyridine **7c** based on docking studies[10] in the ITK binding pocket, as well as an alignment of both compound classes. The main interactions with the protein, that is, the hydrogen-bond interactions with backbone carbonyl

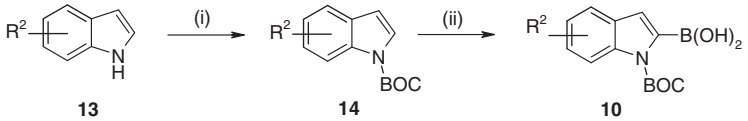

Scheme 4. Reagents and conditions: (i) Boc_2O, NEt_3, DMAP, DMF, 0 °C to rt, 1 h; (ii) $B(OiPr)_3$, LDA, THF, 0 °C, 2 h, argon.

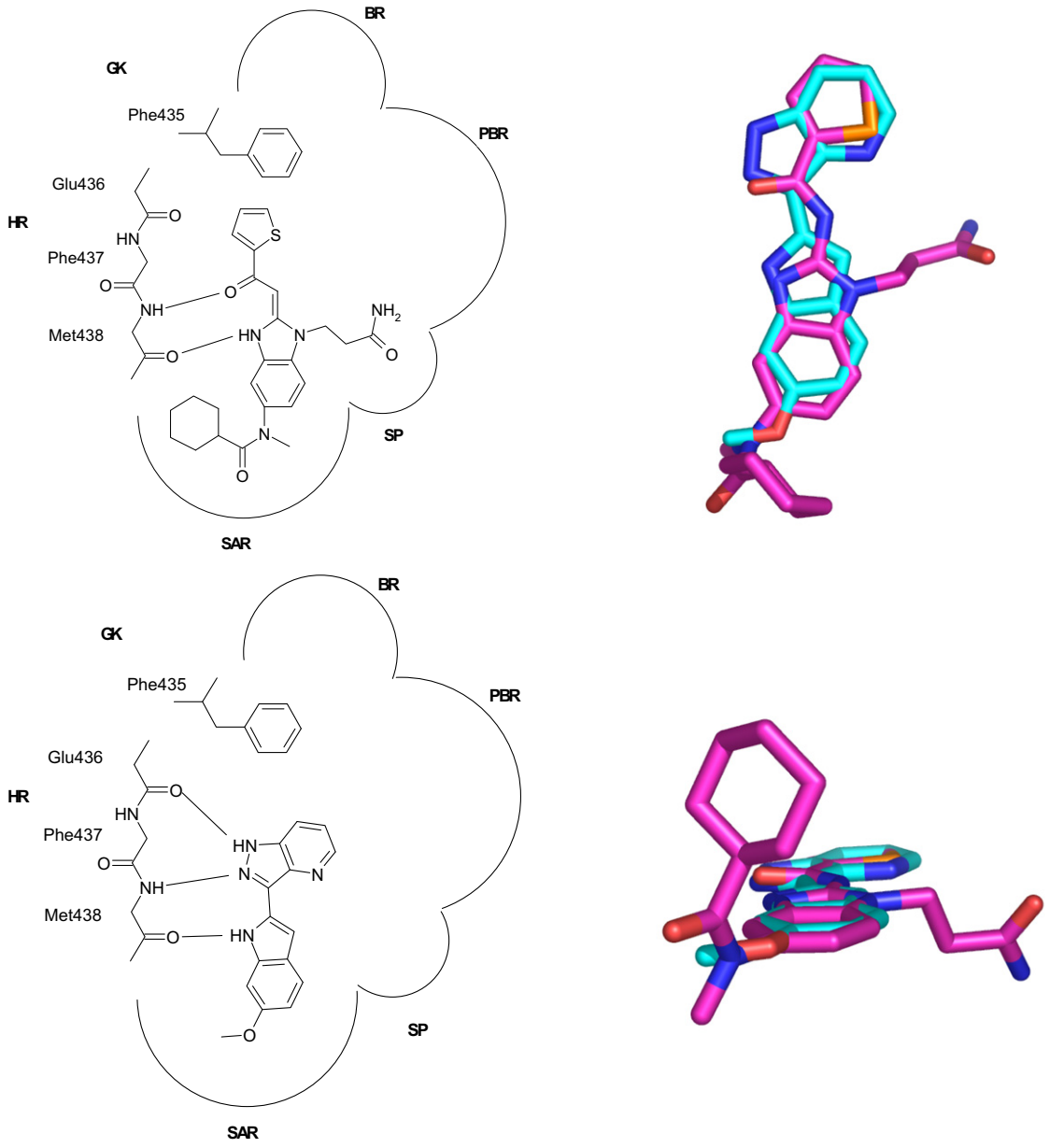

Figure 4. Minimisation of published ITK inhibitor **2** (magenta) and indolylindazole derivative **7c** (cyan) in ITK binding pocket result in the shown alignment of both classes.

oxygen of Glu-436 and backbone nitrogen and oxygen of Met-438 in the hinge region and aromatic and hydrophobic interactions with the gatekeeper Phe-435 are identical for both ITK inhibitors. As the alignment indicates, the methoxy group of **7c** occupies apparently the same space as the methyl amide moiety of benzimidazole **2**.[14] Based on these docking results it appeared that the methoxy group of **7c** could be replaced in further optimisation cycles with larger, sterically more demanding substituents. In order to verify our initial hypothesis that a planar inhibitor scaffold might not only increase ITK binding affinity, but also enhance the selectivity of ITK against CDK2 inhibition, **7c** has also been tested against CDK2 enzyme. In view of initial hit **4a** which inhibited both enzymes almost equipotently (ITK IC_{50} = 5 μM vs CDK2 IC_{50} = 3 μM), the selectivity observed for **7c** was significantly higher than expected. Compound **7c** is almost 70-fold more potent against ITK compared to CDK2 (ITK IC_{50} = 0.06 μM versus CDK2 IC_{50} = 4 μM). Subsequent external profiling of **7c** in a kinase panel applying similar assay conditions[18] confirmed the selectivity with regard to cyclin dependent kinases (Table 3). However, 4 out of 32 kinases tested in the panel were inhibited in the submicromolar range. A modest selectivity was observed with regard to Aurora A, Aurora B and VEGF-R2 (3–5-fold). In addition, the receptor tyrosine kinase FLT3 was inhibited equipotently. Nevertheless, taking into account that **7c** is substituted with one single methoxy group only the observed selectivity profile was considered as encouraging.

In conclusion, ITK inhibitors were designed and synthesized in a focused kinase library approach within iterative cycles. Structural information of the ITK ATP binding pocket supported both the identification of main interactions of first generation libraries with the protein and the successful optimisation of these initial hits in following syntheses. Representative compounds, such as **7c**, are potent against the target enzyme and in a cellular assay. Moreover, they exhibit an excellent ligand efficiency and **7c** showed promising initial selectivity in a panel of about 30 kinases. The identified compound cluster was therefore selected as a main starting point for the ITK lead finding project.

Table 3
Selectivity profiling of compound **7c** in a panel of 32 kinases

Kinase	IC_{50} (μM) enzyme[a,b]	Kinase	IC_{50} (μM) enzyme[a,b]
ABL1	7.68	IKK-beta	—
Aurora A	0.19	MEK-1	2.45
Aurora B	0.27	NEK-2	3.22
B-RAF	—	p38-alpha	—
CDC42 BpB	—	PAK2	—
CDK1/CycB	5.23	PBK	—
CDK2/CycA	5.38	PDGFR-beta	3.20
CDK4/CycD1	1.45	PKC-beta1	—
CDK5/p25	7.41	PKC-theta	22.40
CDK7/CycH1	1.78	PLK1	—
CDK9/CycT	—	S6-Kinase	—
CHK1	5.94	SAK	3.82
CK2-alpha1	—	SRC	1.31
DAPK1	—	TTK	8.75
FAK	5.49	VEGF-R2	0.31
FLT3	0.06	WEE1	5.72

[a] IC_{50} values calculated from a single experiment.
[b] No data: IC_{50} >30 μM.

Acknowledgements

We thank J. Wilsberg, T. Piper and Dr. I. Schlemminger for skilful synthetic support, M. Beschle and K.-M. Nagy for LC–MS purifications, Dr. H.-C. Holst and T. Kottysch for NMR analyses, A. Borkowski, S. Braun, M. Nickel, Dr. M. Schäfer and Dr. T. Ciossek for biological testing.

References and notes

1. (a) Yamada, N.; Kawakami, Y.; Kimura, H.; Fukamachi, H.; Baier, G.; Altman, A.; Kato, T.; Inagaki, Y.; Kawakami, T. *Biochem. Biophys. Res. Commun.* **1993**, *192*, 231; (b) Siliciano, J. D.; Morrow, T. A.; Desiderio, S. V. *Proc. Natl. Acad. Sci. U.S.A* **1992**, *89*, 11194.
2. (a) Schaeffer, E. M.; Debnath, J.; Yap, G.; McVicar, D.; Liao, X. C.; Littman, D. R.; Sher, A.; Varmus, H. E.; Lenardo, M. J.; Schwartzberg, P. L. *Science* **1999**, *284*, 638; (b) Fowell, D. J.; Shinkai, K.; Liao, X. C.; Beebe, A. M.; Coffman, R. L.; Littman, D. R.; Locksley, R. M. *Immunity* **1999**, *11*, 399.
3. Mueller, C.; August, A. *J. Immunol.* **2003**, *170*, 5056.
4. Lin, T. A.; McIntyre, K. W.; Das, J.; Liu, C.; O'Day, K. D.; Penhallow, B.; Hung, C. Y.; Whitney, G. S.; Shuster, D. J.; Yang, X.; Townsend, R.; Postelnek, J.; Spergel, S. H.; Lin, J.; Moquin, R. V.; Furch, J. A.; Kamath, A. V.; Zhang, H.; Marathe, P. H.; Perez-Villar, J. J.; Doweyko, A.; Killar, L.; Dodd, J. H.; Barrish, J. C.; Wityak, J.; Kanner, S. B. *Biochemistry* **2004**, *43*, 11056.
5. Brown, K.; Long, J. M.; Vial, S. C.; Dedi, N.; Dunster, N. J.; Renwick, S. B.; Tanner, A. J.; Frantz, J. D.; Fleming, M. A.; Cheetham, G. M. *J. Biol. Chem.* **2004**, *279*, 18727.
6. (a) Stocks, M. J.; Wilden, G. R.; Pairaudeau, G.; Perry, M. W.; Steele, J.; Stonehouse, J. P. *ChemMedChem* **2009**, *4*, 800; (b) Hann, M. M.; Oprea, T. I. *Curr. Opin. Chem. Biol.* **2004**, *8*, 255.
7. Hopkins, A. L.; Groom, C. R.; Alex, A. *Drug Discovery Today* **2004**, *9*, 430.
8. (a) Abad-Zapatero, C.; Metz, J. T. *Drug Discovery Today* **2005**, *10*, 464; (b) Bembenek, S. D.; Tounge, B. A.; Reynolds, C. H. *Drug Discovery Today* **2009**, *14*, 278.
9. (a) Das, J.; Furch, J. A.; Liu, C.; Moquin, R. V.; Lin, J.; Spergel, S. H.; McIntyre, K. W.; Shuster, D. J.; O'Day, K. D.; Penhallow, B.; Hung, C. Y.; Doweyko, A. M.; Kamath, A.; Zhang, H.; Marathe, P.; Kanner, S. B.; Lin, T. A.; Dodd, J. H.; Barrish, J. C.; Wityak, J. *Bioorg. Med. Chem. Lett.* **2006**, *16*, 3706; (b) Das, J.; Liu, C.; Moquin, R. V.; Lin, J.; Furch, J. A.; Spergel, S. H.; Doweyko, A. M.; McIntyre, K. W.; Shuster, D. J.; O'Day, K. D.; Penhallow, B.; Hung, C. Y.; Kanner, S. B.; Lin, T. A.; Dodd, J. H.; Barrish, J. C.; Wityak, J. *Bioorg. Med. Chem. Lett.* **2006**, *16*, 2411.
10. (a) Gerber, P. R.; Muller, K. M. A. B. *J. Comput. Aided Mol. Des.* **1995**, *9*, 251; (b) www.moloc.ch.
11. (a) Ghose, A. K.; Herbertz, T.; Pippin, D. A.; Salvino, J. M.; Mallamo, J. P. *J. Med. Chem.* **2008**, *51*, 5149; (b) McInnes, C. *Curr. Opin. Drug Discov. Devel.* **2006**, *9*, 339.
12. (a) Kim, K. S.; Kimball, S. D.; Misra, R. N.; Rawlins, D. B.; Hunt, J. T.; Xiao, H. Y.; Lu, S.; Qian, L.; Han, W. C.; Shan, W.; Mitt, T.; Cai, Z. W.; Poss, M. A.; Zhu, H.; Sack, J. S.; Tokarski, J. S.; Chang, C. Y.; Pavletich, N.; Kamath, A.; Humphreys, W. G.; Marathe, P.; Bursuker, I.; Kellar, K. A.; Roongta, U.; Batorsky, R.; Mulheron, J. G.; Bol, D.; Fairchild, C. R.; Lee, F. Y.; Webster, K. R. *J. Med. Chem.* **2002**, *45*, 3905; (b) Misra, R. N.; Xiao, H. Y.; Kim, K. S.; Lu, S.; Han, W. C.; Barbosa, S. A.; Hunt, J. T.; Rawlins, D. B.; Shan, W.; Ahmed, S. Z.; Qian, L.; Chen, B. C.; Zhao, R.; Bednarz, M. S.; Kellar, K. A.; Mulheron, J. G.; Batorsky, R.; Roongta, U.; Kamath, A.; Marathe, P.; Ranadive, S. A.; Sack, J. S.; Tokarski, J. S.; Pavletich, N. P.; Lee, F. Y.; Webster, K. R.; Kimball, S. D. *J. Med. Chem.* **2004**, *47*, 1719; (c) Pevarello, P.; Brasca, M. G.; Orsini, P.; Traquandi, G.; Longo, A.; Nesi, M.; Orzi, F.; Piutti, C.; Sansonna, P.; Varasi, M.; Cameron, A.; Vulpetti, A.; Roletto, F.; Alzani, R.; Ciomei, M.; Albanese, C.; Pastori, W.; Marsiglio, A.; Pesenti, E.; Fiorentini, F.; Bischoff, J. R.; Mercurio, C. *J. Med. Chem.* **2005**, *48*, 2944; (d) Pevarello, P.; Brasca, M. G.; Amici, R.; Orsini, P.; Traquandi, G.; Corti, L.; Piutti, C.; Sansonna, P.; Villa, M.; Pierce, B. S.; Pulici, M.; Giordano, P.; Martina, K.; Fritzen, E. L.; Nugent, R. A.; Casale, E.; Cameron, A.; Ciomei, M.; Roletto, F.; Isacchi, A.; Fogliatto, G.; Pesenti, E.; Pastori, W.; Marsiglio, A.; Leach, K. L.; Clare, P. M.; Fiorentini, F.; Varasi, M.; Vulpetti, A.; Warpehoski, M. *J. Med. Chem.* **2004**, *47*, 3367.
13. (a) Jiang, N.; Ragauskas, A. J. *Tetrahedron Lett.* **2006**, *47*, 197; (b) Beletskaya, I. P.; Ganina, O. G.; Tsvetkov, A. V.; Fedorov, A. Y.; Finet, J.-P. *Synlett* **2004**, 2797.
14. Cook, B. N.; Bentzien, J.; White, A.; Nemoto, P. A.; Wang, J.; Man, C. C.; Soleymanzadeh, F.; Khine, H. H.; Kashem, M. A.; Kugler, S. Z.; Wolak, J. P.; Roth, G. P.; De Lombaert, S.; Pullen, S. S.; Takahashi, H. *Bioorg. Med. Chem. Lett.* **2009**, *19*, 773.
15. *Protein kinase scintillation proximity assay (enzymatic assay):* 150 ng purified recombinant baculovirus-expressed GST-Itk full-length was incubated in 50 μl kinase assay buffer (2 mM MOPS/NaOH, pH 7.0, 5 mM $MgCl_2$, 5 mM $MnCl_2$, 0.5% glycerol, 0.1 mM EDTA, pH 7.4, 1 mM DTT, 0.0001% Brij35, 0.3 mg/ml BSA) containing 0.1 mM ATP, 2 mCi [^{33}P]-ATP and 1,5 μM of biotinylated JAK2 peptide (Biotin-ßAla-ßAla-KTFCGTPEYLAPEVRREPRILSEEEQEMFRDFDYIADWC-NH2) in Wallac Isoplates (Perkin–Elmer). Substrate phosphorylation was measured by incorporation of ^{33}Pi from γ-[^{33}P]-ATP (Amersham). After 30 min at room temperature, the reaction was stopped by adding 150 ml stop solution (10 mM ATP, 1.33 mg/ml streptavidin-coated yttrium silicate beads (Amersham), 5 mM EGTA, pH 7.5, 0.1% Triton X-100). Radioactivity was counted with the Wallac Micro β1450 (Perkin–Elmer).
16. *General procedure for Suzuki coupling and Boc deprotection:* Under argon indazole building block **8** or **9** (0.30 mmol) and boronic acid **10** (0.39 mmol) were dissolved in dioxane (3 mL). Subsequently, 2 M Cs_2CO_3aq (1.2 mmol) and then palladium catalyst $Pd(dppf)_2Cl_2$–DCM (0.015 mmol) were added. The reaction mixture was stirred at 80 °C for 2–4 h. The organic and aqueous layers were separated, the aqueous phase was extracted with AcOEt (2 × 2 mL). The organic phases were filtered over aluminum oxide. After evaporation of the filtrate under reduced pressure the residue was dissolved in MeOH (2 mL). THF (2 mL) and 4 M K_2CO_3aq (2 mL) were added and the mixture was stirred vigorously at 60 °C over 3–4 h. The mixture was condensed under reduced pressure and AcOEt (5 mL) was added. The layers were separated and the aqueous layer was extracted with AcOEt (3 × 5 mL). The combined organic layers were dried over Na_2SO_4 and evaporated under reduced pressure. The crude products were purified either by preparative HPLC (C18, acetonitrile/water at pH 3.75, ammonium formate buffer) or by flash chromatography (silica gel, cyclohexane/AcOEt).
17. *CD4+ T cell assay:* CD4+ T cells were isolated from human whole blood (citrate 0.31% w/v) by Percoll gradient centrifugation followed by negative selection with CD4+ T cell Isolation Kit II (Miltenyi) according to the manufacturer's instructions. CD4+ T cells were seeded 2 × 10^5 cells/well in 96-MTP in RPMI 1640 medium containing 10% heat-inactivated FBS, 2 mM L-Glutamine and 1% penicillin/streptomycin (Gibco). The cells were preincubated with test compounds for 30 min (0.1% DMSO final concentration) and stimulated with 0.3 μg/well plate bound a-CD3 (OKT3, Janssen&Cilag)) and 3 μg/ml α-CD28 (Beckman) for 48 h at 37 °C. 150 μl of the supernatants were collected. The IL2 release was measured by electro-chemiluminescence (Bioveris) according to the manufacturer's protocol using anti-IL2 antibodies from R&D Systems.
18. *Kinase selectivity profiling:* The selectivity of compound **7c** was characterised in a kinase panel test (ProQinase GmbH, Freiburg, Germany). Thirty two kinases were tested in a radiometric [^{33}P] in vitro kinase assay (FlashPlate™) at an ATP concentration of 100 nM. Compound **7c** was applied in dose response curves from 10 nM to 30 μM to calculate IC_{50} values.